 DOI: 10.1002/masy.200751326

Dispersion Polymerization of Methyl Methacrylate in Supercritical Carbon Dioxide: Control of Molecular Weight Distribution by Adjusting Particle Surface Area

Philipp A. Mueller,[1] *Giuseppe Storti,*[2] *Massimo Morbidelli,**[2]
Charalampos A. Mantelis,[3] *Thierry Meyer*[3]

Summary: Experiments of methyl methacrylate dispersion polymerization are carried out in a reaction calorimeter using PDMS-mMA as surfactant. Different stabilizer concentrations from 0 to 10 wt% with respect to monomer have been considered in order to control particle morphology. The analysis by scanning electron microscopy reveals a definite decrease of the total particle surface area at decreasing stabilizer concentration. At the same time, the analysis of the polymer microstructure by gel permeation chromatography shows a trend of the average molecular weight towards smaller values. In particular, a second mode at low molecular weights has been observed leading to bimodal molecular weight distributions. The experimental results are compared with simulation results obtained through a detailed kinetic model developed in previous studies.[1] The key role of the radical exchange between continuous and dispersed phases is confirmed.

Keywords: calorimetry; dispersion polymerisation; molecular weight distribution; polymerization modelling; supercritical carbon dioxide

Introduction

The dispersion polymerization of methyl methacrylate (MMA) in supercritical carbon dioxide ($scCO_2$) has been investigated by many research groups during the last decades.[2–18] Using different types of surfactants, the successful formation of poly(methyl methacrylate) (PMMA) dispersions made of micron-sized spherical particles was reported. Moreover, many of the mentioned studies measured polymerization rates and polymer molecular weights whereas both have been found to be comparable to those typically observed in conventional heterogeneous processes (i.e. emulsion and suspension polymerization).

Mathematical models provided assistance with the disclosure of the underlying process mechanisms. The models developed by Ahmed and Poehlein[19,20] and Saenz and Asua,[21] both designed for dispersion polymerization in liquid organic solvents, considered the polymerization in both phases. The interphase radical transport, a key process in dispersion polymerization, was described by irreversible diffusion from the continuous phase to the polymer particles in both cases. The first comprehensive model of dispersion polymerization in $scCO_2$ has been reported by Chatzidoukas et al.[22] This model is conceptually identical to that proposed by the same group for the suspension

[1] DuPont Engineering Research & Technology, Experimental Station, Wilmington, DE, 19880-0249, USA
[2] Institute for Chemical and Bioengineering, ETH Zurich, Wolfgang-Pauli-Str. 10, CH-8093 Zurich, Switzerland
Fax: (+41) 44 632 1082;
E-mail: massimo.morbidelli@chem.ethz.ch
[3] Groupe of Chemical and Physical Safety, Ecole Polytechnique Fédérale de Lausanne, EPFL-ISIC-GSCP, Station 6, CH-1015 Lausanne, Switzerland

Copyright © 2007 WILEY-VCH Verlag GmbH & Co. KGaA, Weinheim

polymerization of poly(vinyl chloride) whereas the growing radical chains remain segregated in the phase where they were formed.[23]

In a previous contribution[24] we showed that the latter model is unlikely to be applicable for the polymerization system under consideration when using reasonable parameter values and thus prompting us to develop a new model accounting for the detailed description of the radical interphase transport.[25] The so-called Ω-analysis introduced in the same work was focused on the comparison of the characteristic times of termination and interphase mass transport. This analysis showed that in the case of MMA dispersion polymerization in $scCO_2$ a situation of irreversible transport from the continuous phase to the polymer particles prevails. A similar picture is expected for the dispersion polymerization of other conventional monomers such as styrene. On the other hand, a different behavior has been found when polymerizing vinylidene fluoride (VF2) in $scCO_2$ in the absence of a stabilizer (i.e. by precipitation polymerization).[1] Ω-values close to unity (i.e. comparable values of the characteristic times of interphase mass transport and termination for most of the growing chains) have been observed in this case causing a (partly) segregated system which lead to the formation of a polymer with bimodal Molecular Weight Distributions (MWD).

The objective of the present work is to further test and validate the proposed mechanistic picture. In particular, reaction conditions resulting in a partial segregation of the reaction are identified with the model and experiments under such conditions are carried out. This way, it is proved that PMMA with bimodal MWD can be produced by dispersion polymerization in $scCO_2$.

Experimental Part

A set of experiments of MMA dispersion polymerization has been designed to obtain polymer dispersions of largely different morphology. It is well-known that under conditions of effective stabilization of the nucleated polymer phase, a dispersion of equal-sized PMMA spherical particles exhibiting a large interphase surface area can be obtained. On the other hand, in the absence of stabilizing agents (i.e. precipitation polymerization), a bulky phase of amorphous polymer is formed, characterized by very small interphase surface area. Thus, by adjusting the stabilizer concentration in the reactor, it is possible to tune the particle morphology from well-dispersed particles to a bulky phase or, equivalently, the polymer phase surface area from large to small values.

All experiments have been carried out in a stainless steel autoclave coupled to a RC1*e* calorimeter in the laboratories at EPF Lausanne. The detailed reactor setup as well as the polymerization procedure are given elsewhere.[26] The stabilizer used in these runs was poly(dimethlysiloxane) monomethacrylate (PDMS-mMA). Table 1 shows a summary of recipes and conditions of all experiments considered in this work.

Polymerization Model

The model used for the quantitative comparison with the experimental data discussed in the following has originally been developed by Mueller et al.[1,25] It is a comprehensive, generalized kinetic model of heterogeneous polymerization in $scCO_2$,

Table 1.
Recipes and conditions.

$T = 80\ ^\circ C$
$V = 1.3$ L

Run	p_0	$[AIBN]_0$	$[MMA]_0$	$[PDMS\text{-}mMA]_0$
	bar	mol L^{-1}	mol L^{-1}	wt%[a]
A	311	1.18×10^{-2}	1.91	10
B	296	1.17×10^{-2}	1.91	5
C	271	1.20×10^{-2}	1.91	2
D	295	1.19×10^{-2}	1.91	1
E	255	1.14×10^{-2}	1.86	0.75
F	226	1.14×10^{-2}	1.86	0.5
G	259	1.13×10^{-2}	1.86	0.2
H	298	1.18×10^{-2}	1.91	0

[a] with respect to monomer.

Copyright © 2007 WILEY-VCH Verlag GmbH & Co. KGaA, Weinheim

whose main characteristics are as follows: (1) Two reaction loci are considered: the polymer-rich dispersed phase and the CO_2-rich continuous phase. (2) The interphase mass transport is described for all species (i.e. for small molecules as well as for polymeric species). (3) A chain length dependent partition coefficient between continuous and dispersed phase is considered for polymer chains. (4) The process of particle formation or nucleation is not simulated, and a constant number of spherical particles is assumed throughout the entire process. This is because the nucleation period where the particle number changes significantly is expected to be very short in these systems.[15,16]

The interphase equilibrium partitioning of monomer and CO_2 was described by the Sanchez-Lacombe equation of state, whereas a constant partition coefficient has been used for the initiator. Population balance equations have been derived for the radical and terminated chains in both phases and numerically solved using the method proposed by Kumar and Ramkrishna.[27–29] More details about the derivation of the equations and the numerical solution can be found elsewhere.[1,24,25]

All model parameters have been taken from reference[25] without any further adjustment except for the particle surface area A_p. In fact, in polymerization run A, where a stable dispersion of spherical particles with narrow size distribution has been obtained, it is possible to estimate the final particle radius r_p^f from the scanned electron microscopy (SEM) photographs shown in Figure 1. The particle number N_p (which is a model input parameter) is then calculated from the following expression:

$$N_p = \frac{3X^f m^0_{MMA}}{4\pi\rho_{PMMA}(r_p^f)^3}$$

where X^f denotes the conversion at which r_p^f has been evaluated, m^0_{MMA} is the initial monomer mass and ρ_{PMMA} the density of the polymer. Assuming a constant particle number, the total particle surface area A_p is evaluated as a function of conversion as follows:

$$A_p = 4\pi\left(\frac{3V_{pol}}{4\pi N_p}\right)^{2/3} N_p$$

where the volume of the polymer phase, V_{pol}, is a function of conversion and has been estimated accounting for the actual phase composition as predicted by the Sanchez-Lacombe equation of state.

Results and Discussion

The calculated particle radius as a function of monomer conversion is shown in Figure 2. It is worth noting that for runs A and B it was possible to estimate the final value of the average particle radius r_p^f from the SEM photographs in Figure 1. The corresponding values for runs C and D have been estimated through the model by adjusting the total particle surface A_p (i.e. the particle radius r_p^f) in order to optimize the agreement between measured and calculated conversion values (cf. Figure 3). Such values have been obtained by integration of the experimental reaction heat curves from the calorimeter as described in reference.[26] The reliability of such technique has been proved by comparison with off-line measurements carried out by the more conventional gravimetric technique. However, it was not possible to get any calorimetric signal for polymerizations E to H due to reactor fouling: for these reactions the fitting was carried out directly in terms of final MWD (cf. Figure 4).

When using the model in fully predictive way (runs A and B), model results are in good agreement with the experimental observations. On the other hand, a generally good agreement is apparent in terms of conversion and/or MWD for all the other experiments (C to H) when adjusting the particle specific surface. It is then confirmed that the interplay between particle size and polymerization rate is a key peculiarity of the dispersion polymerization in supercritical media: as shown previously,[1,24,25]

Copyright © 2007 WILEY-VCH Verlag GmbH & Co. KGaA, Weinheim

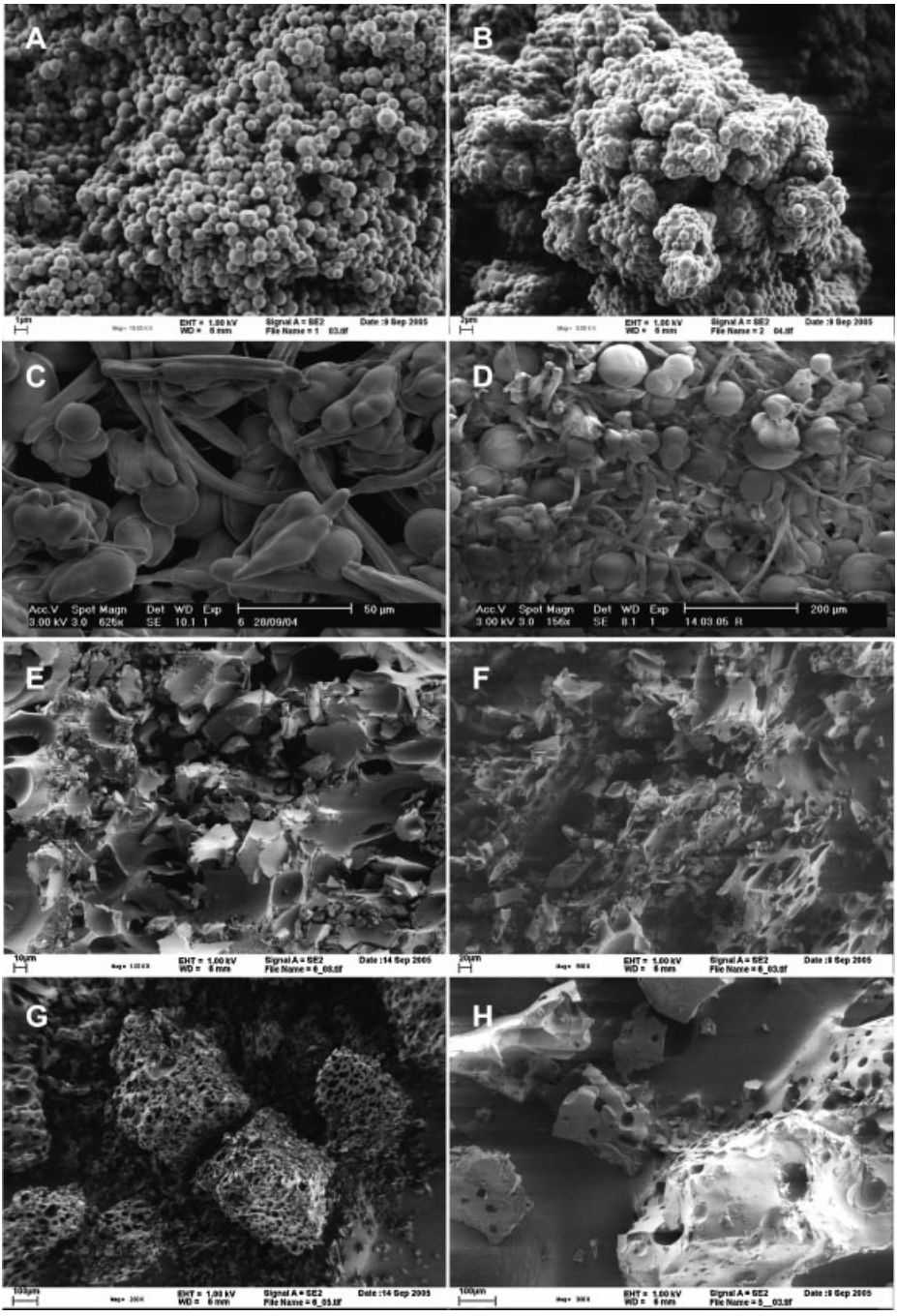

Figure 1.
SEM photographs of PMMA samples obtained from polymerization runs A–H as given in Table 1.

depending on the extent of interphase surface area, the predominant locus of polymerization reaction shifts from the continuous to the dispersed phase. Such shift is clearly shown by the conversion curves for polymerization runs A through H in Figure 3. Notably, the reaction rate is faster in the polymer particles (where gel

Copyright © 2007 WILEY-VCH Verlag GmbH & Co. KGaA, Weinheim

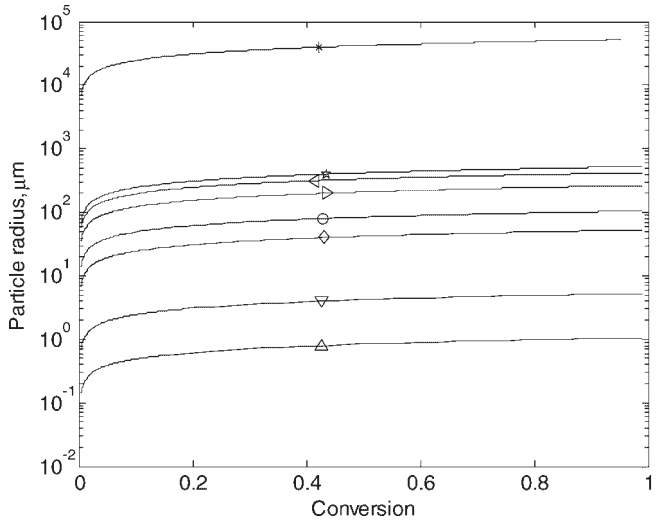

Figure 2.
Calculated particle radius as a function of conversion for polymerization runs A to H; △ = A, ▽ = B, ◇ = C, ○ = D, ▷ = E, = F, ☆ = G, * = H.

effect is also active) than in the continuous phase (slow solution polymerization).

The interplay between particle morphology and polymer microstructure becomes even more evident when looking at the MWD of the polymers produced under conditions A to H as shown in Figure 4. The transition of the dominant polymerization locus from the polymer particles in run A, B, C and D to the continuous phase in run F, G and H is clearly seen by the changing relative importance of the two peaks in the MWD. Under the conditions of run E, it appears that both reaction loci equally contribute to the polymer formation. Model predictions agree well with the

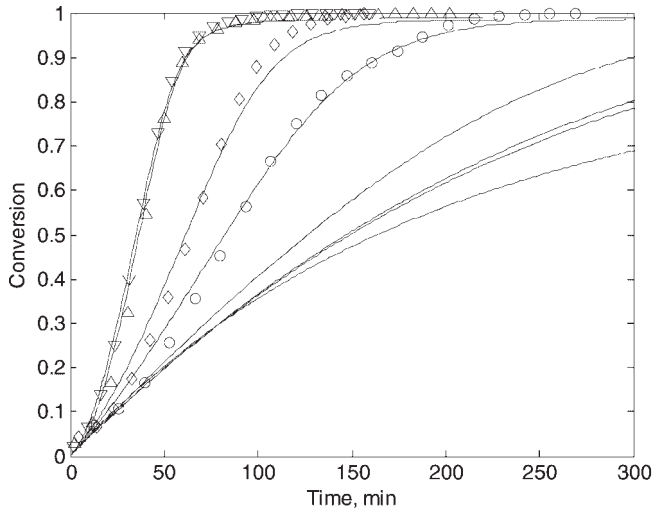

Figure 3.
Calculated (lines) and measured thermal monomer conversion as a function of reaction time; △ = run A, ▽ = run B, ◇ = run C, ○ = run D.

Copyright © 2007 WILEY-VCH Verlag GmbH & Co. KGaA, Weinheim

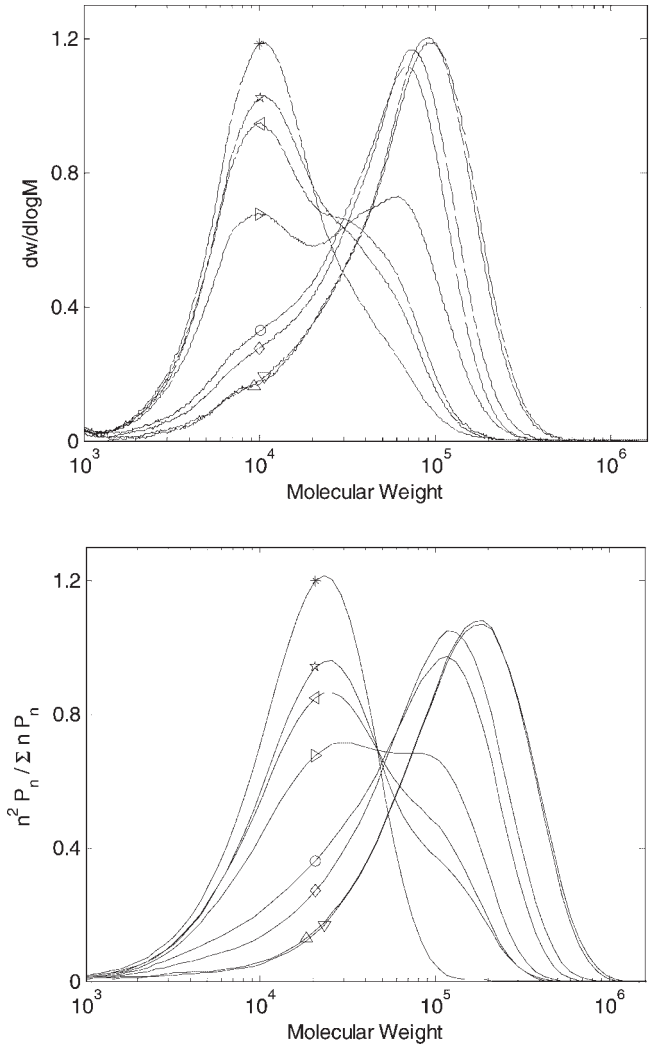

Figure 4.
Experimental (top) and predicted (bottom) MWD for polymerization runs A to H; △ = A, ▽ = B, ◇ = C, ○ = D, ▷ = E, = F, ☆ = G, * = H.

experimental GPC traces. Although the peak maxima are slightly overestimated by the model, their relative weights are captured surprisingly well. These findings strongly confirm the mechanism of the supercritical dispersion polymerization previously proposed.[1,24,25]

Finally, the actual extent of segregation in the polymerization process under examination is estimated. Namely, the so-called Ω parameter is used[1,24,25,30]: it is defined as the ratio between the characteristic time of termination within a given phase and that of mass transport out of the same phase:

$$\Omega_{n,j} = \frac{K_{n,j} A_p}{k_{t,j}[R_{n,j}] V_j}$$

where $K_{n,j}$ is the overall mass transfer coefficient of a chain of length n referred to phase j according to the two-film theory, $k_{t,j}$ the termination rate constant in phase j, $[R_{n,j}]$ the total radical concentration in phase j and V_j the volume of phase j. Accordingly, Ω values much smaller than

Copyright © 2007 WILEY-VCH Verlag GmbH & Co. KGaA, Weinheim

one indicate radical segregation within the phase, that is, the radical terminates inside the phase before being able to diffuse to the other one, whereas in the opposite case, the active chains will diffuse to the other phase before terminating.

The Ω traces at fractional conversion about 0.5 for all the different polymerization runs considered in this work are shown in Figure 5 (1 indicates the continuous phase, 2 the polymer dispersed phase). Each symbol in the figure denotes a single Ω value for a specific chain length and the arrow indicates the direction of increasing chain length. It is important to note that apart from the values for very short oligomers (i.e. the points that exhibit horizontal trend) the Ω values for chains of length of more than a few tens of monomer units rapidly reach an asymptotic value (appearing as a vertical line in Figure 5). Since each trace is changing only slightly with conversion, it is meaningful of the behavior of the entire polymerization run. As expected from the model results discussed above, the asymptotic Ω_1 values of runs A to D are larger than one. In fact, this means that radicals initiated in the supercritical phase will diffuse into the particles rather than terminate in the former. Because the Ω_2 values in the polymer phase are invariably well below one, the entering active chains will most probably further propagate and finally terminate within the particles. This situation leads to the formation of one single population of polymer chains characterized by the conditions prevailing within the polymer phase, as confirmed by the monomodal MWD for runs A to D (cf. Figure 4).[30] On the other hand, Ω_1 values for runs F to H are smaller than one indicating the continuous phase being the main reaction locus in these polymerization runs since radical chains initiated in the continuous phase will not have enough time to diffuse into the polymer particles before terminating in the former. Being produced under solution polymerization conditions, these polymer chains are of low molecular weight. The characteristic Ω_1 value of run E is around unity which means that part of the chains initiated in the supercritical phase will diffuse into the particles and part will terminate in the continuous phase, leading to two populations of comparable weight as confirmed by the bimodal MWD in Figure 4.

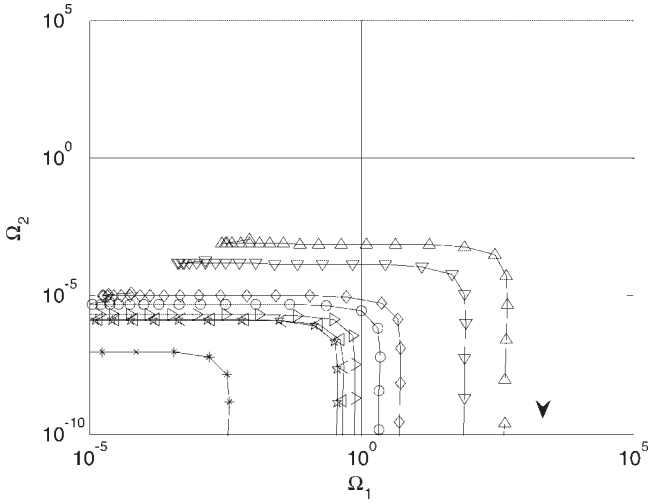

Figure 5.
Omega traces of polymerization runs A to H at around 50% monomer conversion; △ = A, ▽ = B, ◇ = C, ○ = D, ▷ = E, = F, ☆ = G, * = H. Arrow indicates direction of increasing chain length.

Copyright © 2007 WILEY-VCH Verlag GmbH & Co. KGaA, Weinheim

Conclusion

PMMA dispersions of largely different morphologies have been synthesized in scCO2 by adjusting stabilizer concentration. The interplay between particle morphology (i.e. specific surface area) and polymer microstructure has been shown experimentally and analyzed by a comprehensive mathematical model. The good agreement between experimental observations and model results provides a confirmation of the mechanistic picture of supercritical dispersion polymerization reported previously.[24,25]

[1] P. A. Mueller, G. Storti, M. Morbidelli, M. Apostolo, R. Martin, *Macromolecules* **2005**, *38*, 7150–7163.
[2] J. M. DeSimone, E. E. Maury, Y. Z. Menceloglu, J. B. McClain, T. J. Romack, J. R. Combes, *Science* **1994**, *265*, 356–359.
[3] Y. L. Hsiao, E. E. Maury, J. M. DeSimone, S. Mawson, K. P. Johnston, *Macromolecules* **1995**, *28*, 8159–8166.
[4] Y. L. Hsiao, J. M. DeSimone, *J. Polym. Sci. Part A - Polym. Chem.* **1997**, *35*, 2009–2013.
[5] K. A. Schaffer, T. A. Jones, D. A. Canelas, J. M. DeSimone, S. P. Wilkinson, *Macromolecules* **1996**, *29*, 2704–2706.
[6] C. Lepilleur, E. J. Beckman, *Macromolecules* **1997**, *30*, 745–756.
[7] M. L. O'Neill, M. Z. Yates, K. P. Johnston, C. D. Smith, S. P. Wilkinson, *Macromolecules* **1998**, *31*, 2838–2847.
[8] M. L. O'Neill, M. Z. Yates, K. P. Johnston, C. D. Smith, S. P. Wilkinson, *Macromolecules* **1998**, *31*, 2848–2856.
[9] M. Z. Yates, G. Li, J. J. Shim, S. Maniar, K. P. Johnston, K. T. Lim, S. Webber, *Macromolecules* **1999**, *32*, 1018–1026.
[10] P. Christian, M. R. Giles, S. M. Howdle, R. C. Major, J. N. Hay, *Polymer* **2000**, *41*, 1251–1256.
[11] M. R. Giles, J. N. Hay, S. M. Howdle, R. J. Winder, *Polymer* **2000**, *41*, 6715–6721.
[12] P. Christian, S. M. Howdle, D. J. Irvine, *Macromolecules* **2000**, *33*, 237–239.
[13] M. R. Giles, S. J. O'Connor, J. N. Hay, R. J. Winder, S. M. Howdle, *Macromolecules* **2000**, *33*, 1996–1999.
[14] G. Li, M. Z. Yates, K. P. Johnston, S. M. Howdle, *Macromolecules* **2000**, *33*, 4008–4014.
[15] U. Fehrenbacher, O. Muth, T. Hirth, M. Ballauff, *Macromol. Chem. Phys.* **2000**, *201*, 1532–1539.
[16] U. Fehrenbacher, M. Ballauff, *Macromolecules* **2002**, *35*, 3653–3661.
[17] U. Fehrenbacher, M. Ballauff, O. Muth, T. Hirth, *Appl. Organometallic Chem.* **2001**, *15*, 613–616.
[18] M. Okubo, S. Fujii, H. Maenaka, H. Minami, *Colloid Polym. Sci.* **2003**, *281*, 964–972.
[19] S. F. Ahmed, G. W. Poehlein, *Ind. Eng. Chem. Res.* **1997**, *36*, 2597–2604.
[20] S. F. Ahmed, G. W. Poehlein, *Ind. Eng. Chem. Res.* **1997**, *36*, 2605–2615.
[21] J. M. Saenz, J. M. Asua, *Coll. Surf. A: Physiochem. Eng. Aspects* **1999**, *153*, 61–74.
[22] C. Chatzidoukas, P. Pladis, C. Kiparissides, *Ind. Eng. Chem. Res.* **2003**, *42*, 743–751.
[23] C. Kiparissides, G. Daskalakis, D. S. Achilias, E. Sidiropoulou, *Ind. Eng. Chem. Res.* **1997**, *36*, 1253–1267.
[24] P. A. Mueller, G. Storti, M. Morbidelli, *Chem. Eng. Sci.* **2005**, *60*, 377–397.
[25] P. A. Mueller, G. Storti, M. Morbidelli, *Chem. Eng. Sci.* **2005**, *60*, 1911–1925.
[26] C. A. Mantelis, R. Barbey, S. Fortini, T. Meyer, *Macromol. React. Eng.* **2007**, *1*, 78–85.
[27] S. Kumar, D. Ramkrishna, *Chem. Eng. Sci.* **1996**, *51*, 1311–1332.
[28] S. Kumar, D. Ramkrishna, *Chem. Eng. Sci.* **1996**, *51*, 1333–1342.
[29] S. Kumar, D. Ramkrishna, *Chem. Eng. Sci.* **1997**, *52*, 4659–4679.
[30] P. A. Mueller, G. Storti, M. Morbidelli, I. Costa, A. Galia, O. Scialdone, G. Filardo, *Macromolecules* **2006**, *39*, 6483–6488.

Copyright © 2007 WILEY-VCH Verlag GmbH & Co. KGaA, Weinheim